ISSN : 0974 - 7443 Volume 9 Issue 3
CHEMICAL TECHNOLOGY
An Indian Journal
Full Paper
CTAIJ 9(3) 2014 [85-94]

Effect of oxidizing concentration on the corrosion resistance of the cerium conversion coating on galvanized steel

José Daniel Culcasi[1], Cecilia Inés Elsner[1,2], Alejandro Ramón Di Sarli[2]*, Luis Palomino[3], Célia Regina Tomachuk[4], Isolda Costa[4]

[1]Engineering School, National University of La Plata, Av. 1 Esq. 47. CP. B1900TAG, La Plata, (ARGENTINA)
[2]Research and Development Centre in Paint Technology (CICPBA-CCT CONICET LA PLATA); Av. 52 s/n entre 121 y 122. CP. B1900AYB, La Plata, (ARGENTINA)
[3]Polytechnic School of the University of San Pablo (EPUSP), Engineering Chemistry Department, Av. Prof. Lineu Prestes, 580, Caixa Postal 61548, CEP 05508-970, São Paulo-SP, (BRAZIL)
[4]Energy and Nuclear Research Institute, IPEN/CNEN-SP, CCTM, Av. Prof. Lineu Prestes, 2242, CEP 05508-000, São Paulo, SP, (BRAZIL)
E-mail: ardisarli@cidepint.gov.ar; ardisarli@gmail.com; cielsner@ing.unlp.edu.ar; tomazuk@gmail.com

ABSTRACT

Ce-based conversion films have been assessed as alternatives for replacement of Cr^{6+}-based films, which have been forbidden for their toxicity and carcinogenic properties. However, corrosion protection associated with chromate films is difficult to achieve by other surface treatments. Experimental results have revealed that to obtain the highly satisfactory results provided by chromate-based conversion coatings, it is necessary to improve the anticorrosive properties of the new chromium-free coatings. The present work deals with the effect of the oxidant concentration in the cerium-based conversion baths on the corrosion resistance of the films deposited on galvanized steel. Electrogalvanized steel sheets were exposed to cerium chloride-based baths with different concentrations of oxidant for a minute. The surface of the treated samples was analyzed by XPS and SEM-EDXS, while its corrosion resistance was investigated using electrochemical tests (EIS) conducted in a 0.05 M NaCl solution and the impedance spectra evolution analyzed as a function of the exposure time. The results showed a direct relationship between oxidant concentration and corrosion resistance. When the oxidant concentration rose from 2 $mL.L^{-1}$ to 12 $mL.L^{-1}$, the corrosion resistance increased about 5 times, and this was attributed to the decrease in the Ce^{3+}/Ce^{4+} relationship of the conversion film.

KEYWORDS

Galvanized steel;
Ce-based conversion films;
Corrosion;
EIS;
SEM;
EDXS;
XPS.

INTRODUCTION

Conversion coatings are used not only to impart corrosion protection but also to improve adhesion of paint systems/ metal surface. Chromate-based conversion coatings composed of Cr^{6+} and Cr^{3+} oxides and hydroxides have been used in industry for over 50 years. However, Cr compounds are extremely dangerous for human health and generate serious problems of environmental contamination. In particular, and appealing

to increasingly restrictive measures regarding effluent discharge, handling of specimens with chromic treatments and exposure of workers to sprays, pressures on the industrial sector to eliminate the use of Cr compounds have lately become stronger[1,2]. Consequently, investigation of new passivation processes as alternatives for replacement of Cr^{6+}[3] is needed. Rare earth-based conversion coatings have been reported as one of a number of alternatives. Among them, formulations such as cerium nitrate ($Ce(NO_3)_3$), cerium perchlorate ($Ce(ClO_4)_3$) and cerium chloride ($CeCl_3$), have been applied on a range of metals including aluminum, magnesium, tin and zinc alloys.

In earlier works, conversion coatings were obtained by immersion of the metal in cerium salt for a long period of time[4-16]. Lately, the process has been accelerated by acidifying the solution and adding hydrogen peroxide (H_2O_2). The addition of an oxidant and the acidification of the solution allowed conducting the process in a reasonable period of time (< 10 min)[5,17-24]. Electrolytic deposition[13,16,25-27], spray[23,28-30], sol-gel process[31-34] and co-deposition with a polymer[35] are among the Ce-based passivation methods used.

Aramaki conducted several studies on corrosion of passivated Zn on films containing Ce and exposed to 0.5 M NaCl solutions[7,9,18,35-37]. This author determined that during immersion in a Cr^{3+} salt (nitrate or chloride), a thin film (~50 nm) of hydrated or hydroxilated Ce_2O_3 containing a small amount of Ce^{+4}, derived from Ce^{3+} oxidation with hydrogen peroxide H_2O_2, is formed on the Zn layer. Such oxidation reaction took place at the cathodic sites as follows:

$$O_2 + 2H_2O + 2e^- \rightarrow H_2O_2 + 2OH^- \quad (1)$$

$$2Ce^{3+} + H_2O_2 \rightarrow 2Ce^{4+} + 2OH^- \quad (2)$$

According to Aramaki, the hydrated or hydroxilated Ce_2O_3 layer grew quickly on the zinc surface by direct reactions on the hydroxilated surface, [Zn]OH with partially hydroxilated or hydrated Ce^{3+} ions, as for example:

$$[Zn]OH + Ce(III)OH \rightarrow [Zn]OCe(III)OH + H^+ \quad (3)$$

$$[Zn]OCe(III)OH + Ce(III)OH \rightarrow [Zn]OCe(III)OCe(III)OH + H^+ \quad (4)$$

$$2[Zn]OCe(III)OH \rightarrow [Zn]OCe(III)(OH)OCe(III)O[Zn] + H^+ \quad (5)$$

Repeated reactions would lead to the formation of the Ce_2O_3 film[38-40]. This film would prevent the cathodic process of zinc corrosion by acting as a barrier against the oxygen diffusion. However, this layer has no self-healing activity, therefore, to suppress the anodic process in scratched areas of the zinc surface is necessary to modify the Ce-based film by different procedures. In this sense, the usage of H_2O_2 generates a film containing a higher amount of Ce^{4+} ions that improves the protective ability of the hydrated cerium oxide[18].

Scholes et al.[17] propose that the addition of H_2O_2 to the solution forms peroxo-cerium $Ce(H_2O_2)^{3+}$ complexes, which evolve by deprotonation and oxidation towards insoluble species such as $Ce^{4+}(O_2)(H_2O_2)^{3+}$. This precipitates forming CeO_2 nanocrystals, whose size decreases as the H_2O_2 concentration increases.

The aim of the present work was to study the anticorrosion effect of the H_2O_2 concentration in $CeCl_3$ solutions used in the passivation treatment of electrogalvanised steels exposed to the action of 0.05 M NaCl solution.

EXPERIMENTAL

Materials and samples preparation

Panels of electrogalvanised steel were passivated by Ce-based conversion films obtained from the solutions indicated in TABLE 1, and according to the following procedure: 1) removal of the original Zn coating by consecutive immersion in three cubes containing 1:1 de HCl solution; 2) rinse with flowing tap water; 3) anodic degreasing at room temperature by using 20% ST 190® + 10% ST 091® solution for 5 min, current density 3 $A.dm^{-2}$; 4) rinse with flowing tap water; 5) activation in 5% Prepalloy® for 30 s; 6) rinse with flowing tap water; 7) electrogalvanised in SurTec 704® bath (KOH- based), current density 3.25 $A.dm^{-2}$, and voltage 3.5 V for 45 min; 8) rinse with flowing tap water; 9) activation in 1% HNO_3 solution for 15 s; 10) rinse with flowing tap water; 11) activation in NaHO solution (pH = 12.85) for 15 s; 12) rinse with flowing tap water; 13) immersion in one of the conversion baths depicted in TABLE 1 at 23±2 ºC for 1 min; 14) rinse with flowing tap water; 15) drying in hot air

Characterization methods

The surface of the samples before and after the elec-

trochemical impedance analysis was analyzed by scanning electronic microscopy and energy dispersive X-ray spectroscopy. The analyses were conducted in a Philips SEM 505 scanning electronic microscope, with Images Digitalizer Soft Imaging System ADDA II and analytical capacity through the EDAX DX PRIME 10 Microwave System with ultrathin window (UTW).

TABLE 1 : Conversion baths concentration

Bath	$CeCl_3$ [g.L^{-1}]	H_2O_2 [mL.L^{-1}]	H_3BO_3 [g.L^{-1}]	pH
A	2.40	2.00	0.02	3.80
B	2.40	5.00	0.10	3.20
C	2.40	8.00	0.10	3.21
D	2.40	12.00	0.10	3.18

The conversion films composition was analyzed by X-ray photoelectron spectroscopy (XPS). The spectra were taken by exciting with 1253.6 eV radiation (Mg Kα, non-monochromatic), anodic voltage 13 kV, and power 300 W, by means of a PHOIBOS 100 MCD, SPECS Hemispheric Energy Analyzer, operating with a pass energy of 40 eV for broad spectra and regions used for quantification, and 10 eV for the region of Ce 3d high resolution used for the deconvolution and calculation of the Cr^{3+}/Cr^{4+} ratios. The spectra were obtained in the initial stage and after scrape each sample with Ar^+ bombardment (3 keV) for 15 and 30 min. The quantification was conducted by assuming that the present elements were homogenously distributed in the entire samples surface. The calculation of the Cr^{3+} and Cr^{4+} percentages was conducted from the deconvolution of the Ce $3d_{3/2}$ transition by using the components indicated in TABLE 2[39,41]:

TABLE 2 : Components of the XPS spectrum corresponding to Ce3d

Ce $3d_{5/2}$	v_0 (Ce^{III})	v (Ce^{IV})	v´ (Ce^{III})	v´´ (Ce^{IV})	v´´´ (Ce^{IV})
Ce $3d_{3/2}$	u_0 (Ce^{III})	u (Ce^{IV})	u´ (Ce^{III})	u´´ (Ce^{IV})	u´´´ (Ce^{IV})

The Ce(III) porcentage was calculated as follows:

$\%Ce(III) = (u_0+u´)/(u_0+u+u´+u´´+u´´´)$

Electrochemical tests

The shielding performance of each coating applied on the steel sheets and subjected to continuous immersion in open to the air 0.05 M NaCl solution was studied by EIS measurements carried out using a conventional electrochemical cell with the three-electrodes arrangement: a Pt wire with negligible impedance acting as counter electrode, a Saturated Calomel Electrode (SCE) was used as reference electrode, and the working electrode was the coated steel sample, placed horizontally looking upwards at the bottom in a flat-cell configuration. The electrolytes were confined in glass tubes attached to the working electrode by an o-ring defining a nominal testing area = 1.77 cm^2. All the measurements were performed at room temperature (22±3 °C).

Impedance spectra in the frequency range $10^{-2} < f(Hz) < 10^5$ were obtained, in the potentiostatic mode at the open circuit potential (OCP), as a function of the immersion time in the electrolyte solution using a Solartron 1250 frequency response analyzer connected to an EG&G 273A potentiostat and both controlled by the ZPlot® program. The rms width of the sinusoidal voltage signal applied to the system was 8mV, and 10 points per decade were registered. All impedance measurements were executed with the electrochemical cell inside a Faraday cage to reduce external interferences as much as possible. The samples integrity was checked by measuring the corrosion potential after all the tests to confirm that the change from the initial value was no higher than ± 5 mV.

The samples' performance was monitored for 4 days. Between one and the next measurement was allowed to elapse 1 h for the first 8 h of exposure to the salt solution, and then 12, 18, 24, 48, 72 and 96 h.

Taking into account that the corrosion behavior of passivated, painted and/or multi coated materials strictly depends on the production procedure, all the tests were carried out on three replicates of each sample type and the average results obtained for them are the reported in the following Tables and Figures.

RESULTS AND DISCUSSION

SEM-EDXS analyses

Figure 1 shows EDXS spectra of the samples prior to electrochemical impedance tests. The spectra show that the amount of Ce included in the conversion coating slightly increases as the H_2O_2 concentration in the bath is increased.

Figure 2 illustrates SEM images of the samples' sur-

Full Paper

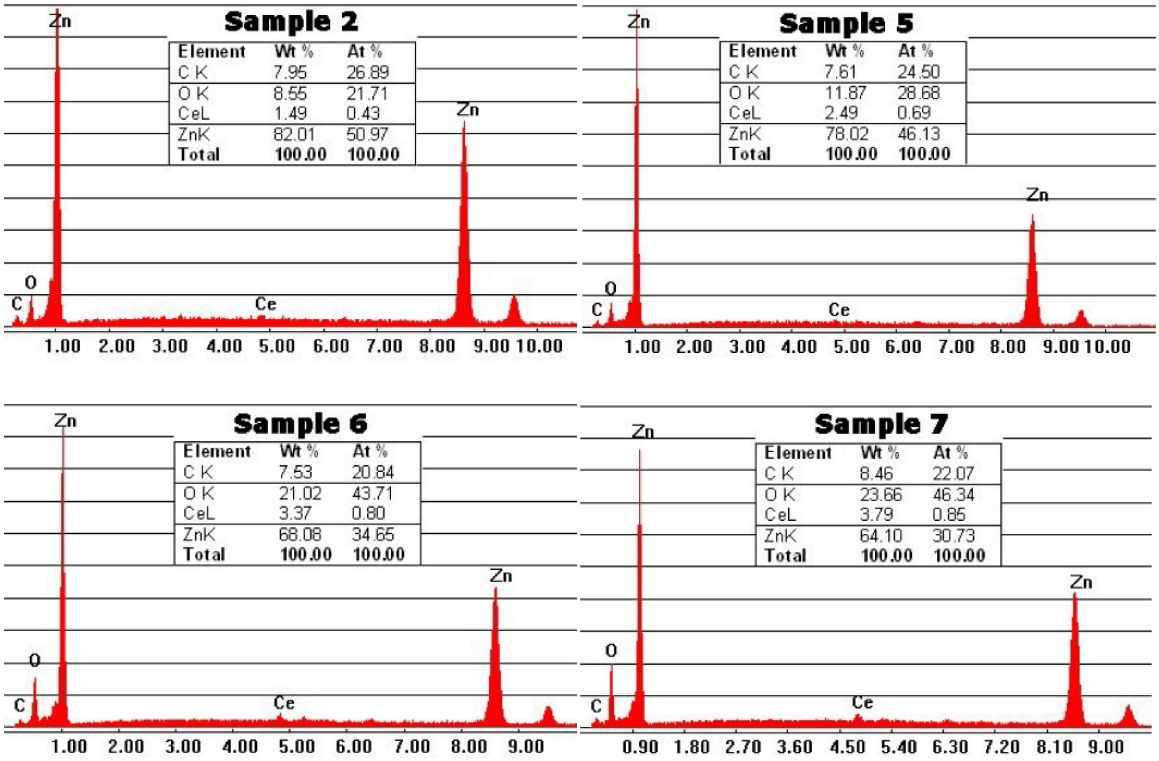

Figure 1 : EDXS spectra of passivated samples

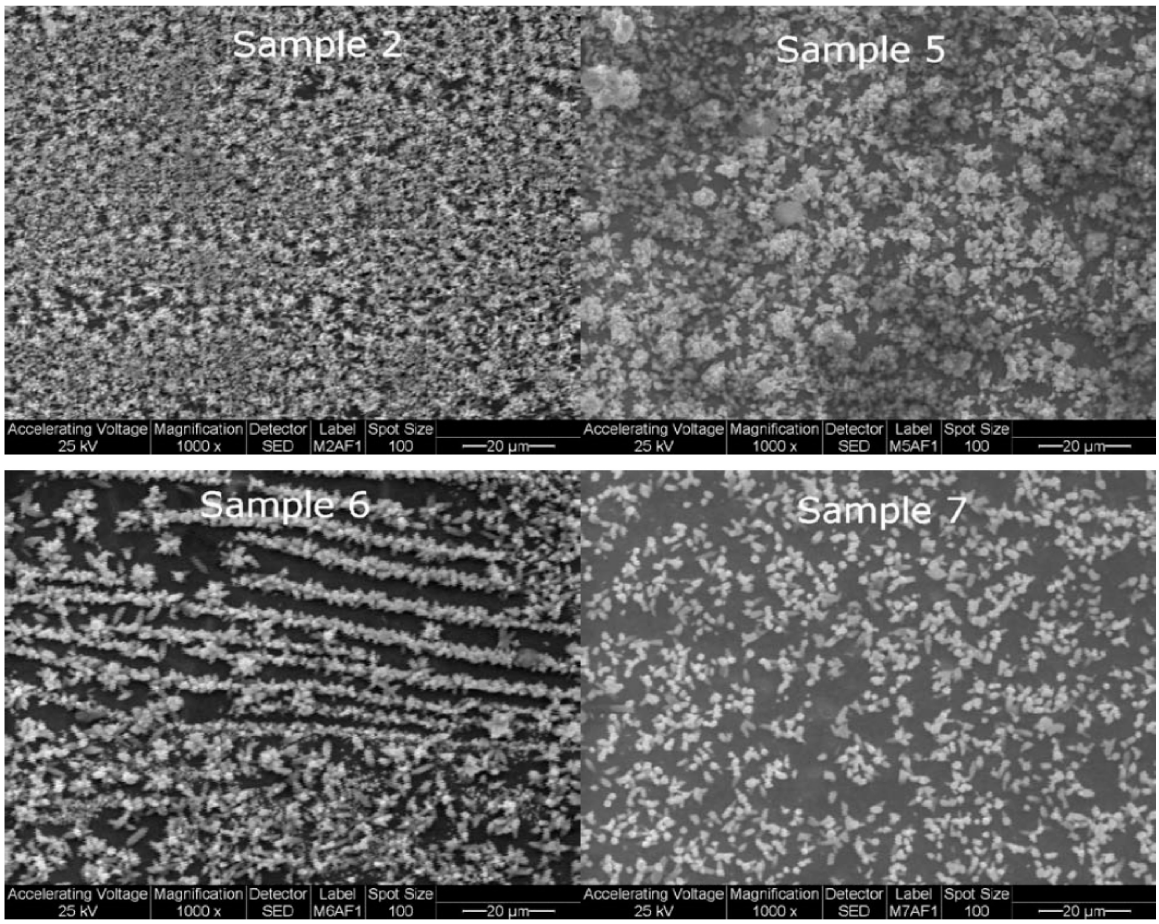

Figure 2 : SEM images of passivated samples after 120 h immersion in 0.05 M NaCl solution

face analyzed after their contact with the aerated 0.05 M NaCl solution for 120 h. It is seen that the amount of corrosion products deposited on those samples decreased as the H_2O_2 concentration increases in the passivating bath.

XPS analysis

Figure 3 exhibits X-ray photoelectron spectra of components Zn 2p, O 1s, and Ce3d for the surface of sample 2 treated in the bath A at 22±3 ºC for 1 min. The depth profiles of the components are indicated with the sputtering time (t_s) in the figure. As seen, these spectra indicate that initially the carbon coming from contamination was the predominant surface element, but also that as more superficial layers were eliminated through repetitive Ar+ bombardments, the amount of carbon decreased and the components corresponding to cerium, zinc and oxygen were more visible. The other three samples showed similar spectra.

A small peak of Zn^{2+} (hydroxide) appeared at ≈ 1023 eV of the binding energy at t_s = 0 min, and an intense peak of Zn^0 emerged at ≈ 1021 eV at $t_s \geq 15$ min in the spectra of Zn $2p_{3/2}$.

There was a peak of O^{2-} at ≈ 530 eV in the spectra of O 1s, whose intensity increased as the t_s did it. Some peaks of Ce^{3+} and Ce^{4+} appeared in the regions of the binding energy between 870 and 925 eV, whose intensity also increased with the t_s in the spectra of Ce $3d_{5/2}$ and Ce $3d_{3/2}$. As well, an increasing satellite peak of Ce^{4+} (u''' peak) was detected in the region between 916 and 920 eV in the Ce $3d_{3/2}$, indicating the presence of a small amount of Ce^{4+} in the layer[42,43].

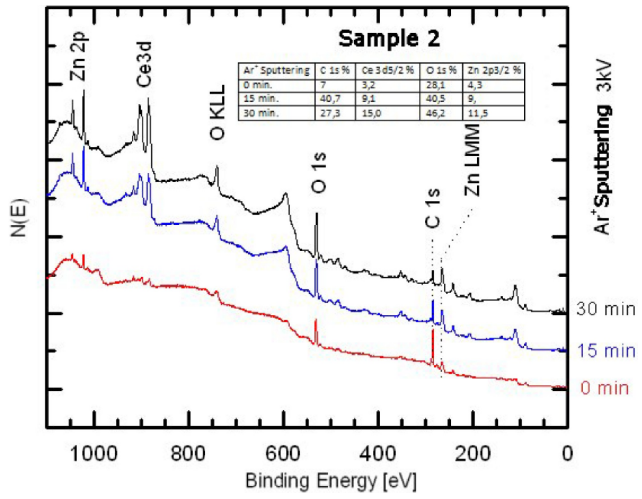

Figure 3 : XPS spectra of sample 2

In order to define the peaks in the Ce 3d spectra, the intensity of the peaks in the spectra at t_s = 0, 15 and 30 min was enlarged for samples 2, 5 and 6, Figure 4. The intensity of the satellite peak at 917 eV increased with the t_s, indicating that an increasing amount of Ce^{4+} was included in the internal parts of the Ce_2O_3 layer as the wear out of the superficial layer increased. Other peaks corresponding to the Ce 3d components of the same samples used to calculate the percentage of Ce^{3+} in the cerium conversion coating are observed at 881.4, 882.8, 866.1, 899.3, 901.6, 904.7, and 907 eV.

As well, it can be seen that as the H_2O_2 concentration increases the u, u´´ and u´´´ components (corresponding to Ce^{4+}) also do it compared with those (u_0 and u´) corresponding to Ce^{3+}.

TABLE 3 indicates that the Ce^{3+}/Ce^{4+} ratio (R) increased with the time of bombardment (t_s) but decreased as the H_2O_2 concentration in the passivating solution increased. These results implied that the content of Ce^{4+} in the conversion coating was higher at the outermost part of the layer than at the inside part.

TABLE 3 : Ce(IV) to Ce(III) ratio

Time of Bombardment with Ar^+ (min)	Sample 2		Sample 5		Sample 6	
	% Ce (III)	% Ce (IV)	% Ce (III)	% Ce (IV)	% Ce (III)	% Ce (IV)
0	31.50	68.50	-----	-----	0.00	100.00
15	72.60	27.40	52.80	47.20	44.90	55.10
30	74.60	25.40	61.20	38.80	46.90	53.10

Electrochemical impedance

The electrochemical impedance spectra as a function of the exposure time corresponding to electrogalvanised steel samples either unpassivated (control) or treated with one of the different passivating baths (sample 2 corresponds to bath A, sample 5 to bath B, sample 6 to bath C, and sample 7 to bath D) are shown as Nyquist diagrams in Figure 5.

As it can be seen, the impedance increases in the unpassivated sample with the exposure time up to 12 h, but decreases markedly after that period. The initial increase in the impedance was attributed to the formation and growth of a relatively steady film of Zn oxide from the anodic (Zn dissolution) and cathodic (oxygen reduction) reactions taking place at defects of the layer

Full Paper

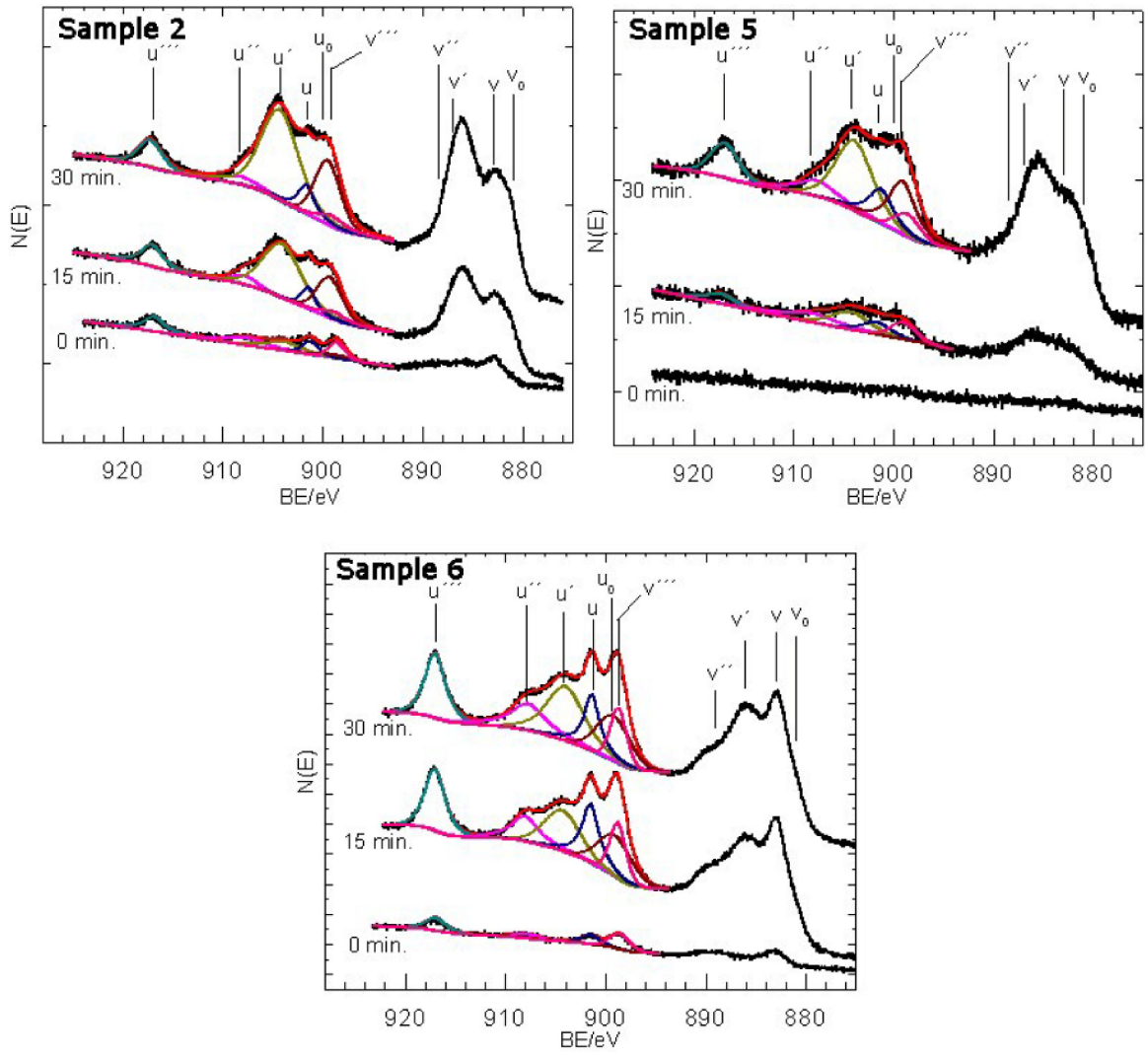

Figure 4 : XPS spectra of the Ce3d component

and over the surface, respectively:

$$Zn \rightarrow Zn^{2+} + 2e^- \quad (6)$$

$$O_2 + 2H_2O + 4e^- \rightarrow 4OH^- \quad (7)$$

As a consequence of the same, zinc hydroxide precipates on the surface and changes to zinc oxide gradually forming a passive layer, which can improve, at this stage, the corrosion resistance by acting as a barrier against the diffusion of the aggressive agents (particularly Cl ions) from the electrolyte's bulk to the metal surface[44]:

$$Zn^{2+} + 4OH^- \rightarrow Zn(OH)_2 + ZnO + H_2O \quad (8)$$

However, because Cl^- accumulates at defects of the passive film and reacts with $Zn(OH)_2$ forming soluble Zn^{2+}–Cl^-–OH^- complexes, the passive film is broken down and local Zn dissolution occurs there[45,46], in such a way that the film formation rate became lower than the dissolution one, generating a decrease in the film thickness and, therefore, in its protective ability.

The sample treated with bath A shows that although after 1 h of exposure the impedance value is similar to that of the control sample, the subsequent increase is much lower but the reduction is produced after 48 h of exposure. This difference in the behavior was attributed to the fact that being the kinetics of Zn oxidation slower due to the passivating effect of Ce, the growth and protective ability of the Zn oxide film and the rate of Zn dissolution are slightly lower, but their protective effect lasts longer.

All the samples treated with the passivating solutions show that as the H_2O_2 concentration increases in the bath the impedance value does it in such a way that this latter was almost 5 times greater in the sample treated with the solution D than in the sample treated

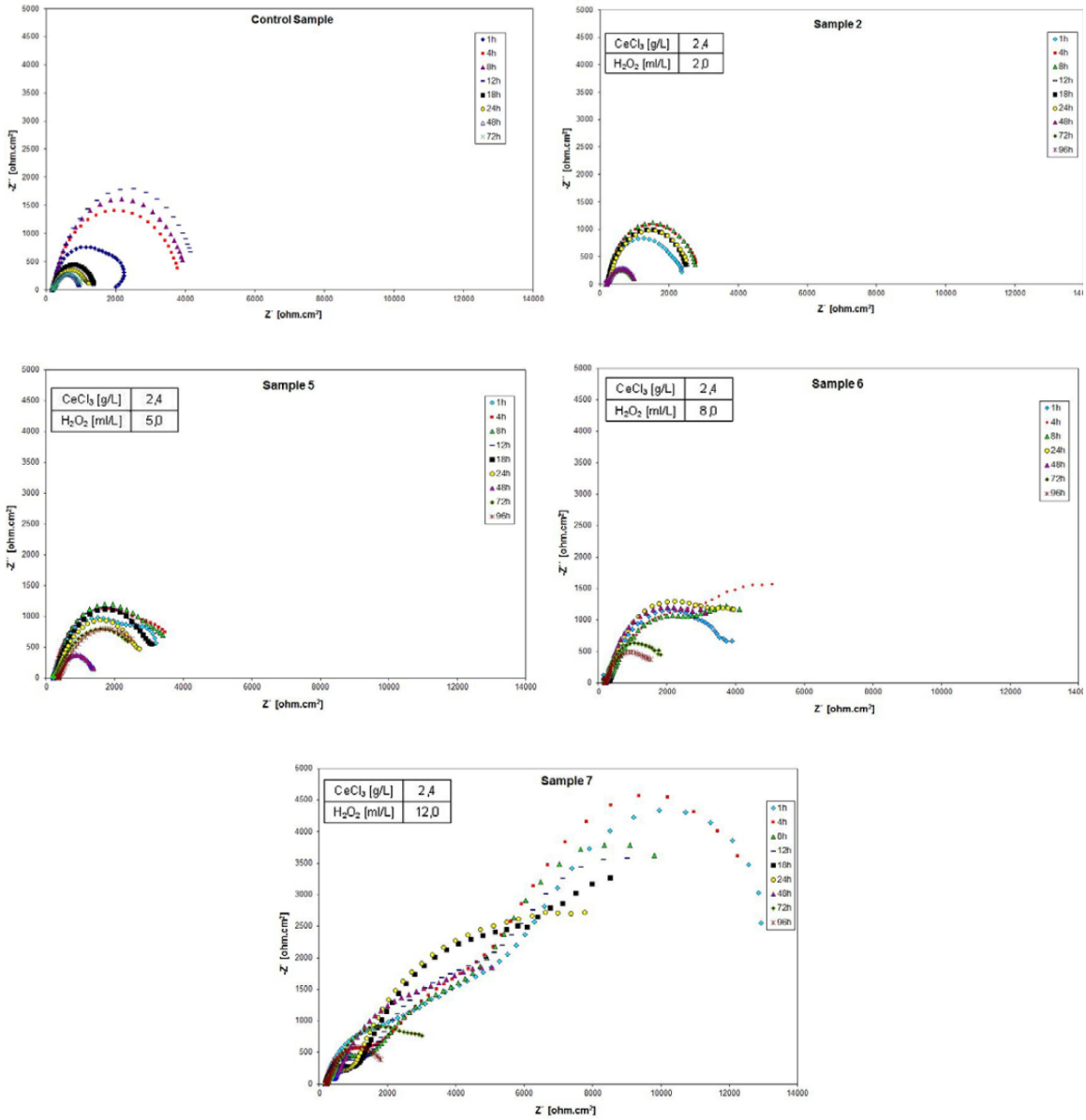

Figure 5 : Electrochemical impedance spectra.

with the solution A. This significant increase in the impedance is indicative of a better protective layer against the zinc corrosion, and it was attributed to the addition of effects such as higher thickness of the passivating film and the increase in the Ce^{4+} proportion in the film deposited on the Zn layer. This evidence, in agreement with the SEM images (Figure 2), confirms the development of a progressive decreasing in the electrochemical surface reactivity. Hence, it was concluded that the protective ability of the hydrated Ce_2O_3 layer against the zinc corrosion in aerated 0.05 M NaCl solution during the immersion was remarkably improved by increasing the solution H_2O_2 concentration. On the other hand, as this concentration in the bath increases, the appearance of more time constants is observed indicating that, despite its passivating effect, the metal surface in contact with the electrolyte is still electrochemically reactive and, therefore, it is subject to lasting variations in the kinetics and/or mechanisms of the physicochemical processes affecting it.

CONCLUSIONS

The effect of an increasing H_2O_2 concentration on the protective capacity of a Ce-based layer against the zinc corrosion in aerated 0.05M NaCl solution for a

number of hours was studied. From the analysis of all the experimental results could be inferred that:

1 The corrosion resistance determined from the impedance values, increased considerably with increasing H_2O_2 content.
2 The Cerium content determined by EDXS increased slightly with the increasing of H_2O_2 content in the bath.
3 The amount of corrosion products formed after 120 h immersion in aerated 0.05 M NaCl solution decreased with increasing H_2O_2 content.
4 Ce^{3+}/Ce^{4+} relationship in the conversion film decreased with the H_2O_2 content in the treatment solution. This ratio was lower in the surface than in the inner part of the sample.

ACKNOWLEDGEMENTS

This research was financed by the CAPES/ MINCyT (Project 158/09 of Brazil and BR/08/04 of Argentina), the Comisión de Investigaciones Científicas de la Provincia de Buenos Aires (CICPBA), the Consejo Nacional de Investigaciones Científicas y Técnicas (CONICET), and the La Plata University of Argentina.

REFERENCES

[1] Chromium (VI) Used in the Coil Coating Industry/ Situation Regarding Health, Safety And Environmental Aspects, ECCA TC 11 Project Team, Chrome Coverage, **(2004)**.
[2] EPA Federal Register, National Emission Standards for Hazardous Air Pollutants For Source Categories: Aerospace Manufacturing And Rework Facilities, **60(170)**, 45947, September **(1995)**.
[3] R.L.Twite, G.P.Bierwagen; Review of alternatives to chromate for corrosion protection of aluminum aerospace alloys, Prog.Org.Coat., **33**, 91–100 **(1998)**.
[4] D.R. Arnott, N.E.Ryan, B.R.W.Hinton, B.A.Sexton, A.E.Hughes; Auger and XPS studies of cerium corrosion inhibition on 7075 aluminum alloy, Appl.Surf.Sci., **236**, 22–23 **(1985)**.
[5] M.Dabalà, L.Armelao, A.Buchberger, I.Calliari; Cerium-based conversion layers on aluminum alloys, Appl.Surf.Sci., **172**, 312–322 **(2001)**.
[6] S.Böhm, R.Greef, H.N.McMurray, S.M.Powell, D.A.Worsley; Kinetic and mechanistic studies of rare earth-rich protective film formation using in situ ellipsometry, J.Electrochem.Soc., **147**, 3286–3293 **(2000)**.
[7] K.Aramaki; Preparation of self-healing protective films on a zinc electrode treated in a cerium(III) nitrate solution and modified with sodium phosphate and cerium(III) nitrate, Corros.Sci., **46**, 1565–1579 **(2004)**.
[8] M.Hosseini, H.Ashassi-Sorkhabi, H.A.Yaghobkhani Ghiasvand; Corrosion protection of electro-galvanized steel by green conversion coatings, J.Rare Earths, **25**, 537–543 **(2007)**.
[9] K.Aramaki; A self-healing protective film prepared on zinc by treatment in a $Ce(NO_3)_3$ solution and modification with $Ce(NO_3)_3$, Corros.Sci., **47**, 1285–1298 **(2005)**.
[10] G.Bikulčius, A.Ručinskienė, A.Sudavičius, V.Burokas, A.Grigucevičienė; Cerium–Permanganate conversion coatings for a Zn–Co alloy, Surf.Coat.Technol., **203**, 115–120 **(2008)**.
[11] G.Wu, Ch.Wang, Q.Zhang, P.Kang; Characterization of Ce conversion coating on Gr-f/6061 Al composite surface for corrosion protection, J.Alloys and Compounds, **461**, 389–394 **(2008)**.
[12] W.G.Fahrenholtz, M.J.O'Keefe, H.Zhou, J.T.Grant; Characterization of cerium-based conversion coatings for corrosion protection of aluminum alloys, Surf.Coat.Technol., **155**, 208–213 **(2002)**.
[13] Sh.N.Lumpp; Obtenção de filmes passivantes de molibdato de amônio e nitrato de cério para ligas de zinco eletrodepositadas, Tesis doctoral Universidade Estadual de Campinas, Brasil, **(2005)**.
[14] M.C.Gonçalves dos Santos; Avaliação do desempenho de filmes contendo silanos e sais de terras raras para proteção contra corrosão de camadas de ZnFe eletrodepositadas, Tesis doctoral Universidade Estadual de Campinas, Brasil, **(2009)**.
[15] M.F.Montemor, A.M.Simoes, M.G.S.Ferreira, M.J.Carmezim; Composition and corrosion resistance of cerium conversion films on the AZ31 magnesium alloy and its relation to the salt anion, Appl.Surf.Sci., **254**, 1806–1814 **(2008)**.
[16] B.R.W.Hinton, D.R.Arnott, N.E.Ryan; Cerium conversion coatings for the corrosion protection of aluminium, Mater.Forum, **9**, 162-173 **(1986)**.
[17] F.H.Scholes, C.Soste, A.E.Hughes, S.G.Hardin, P.R.Curtis; The role of hydrogen peroxide in the deposition of cerium-based conversion coatings,

Appl.Surf.Sci., **253**, 1770–1780 **(2006)**.
[18] K.Aramaki; The effect of modification with hydrogen peroxide on a hydrated cerium(III) oxide layer for protection of zinc against corrosion in 0.5 M NaCl, Corros.Sci., **48**, 766–782 **(2006)**.
[19] B.E.Rivera, B.Y.Johnson, M.J.O'Keefe, W.G.Fahrenholtz; Deposition and characterization of cerium oxide conversion coatings on aluminum alloy 7075-T6, Surf.Coat.Technol., **176**, 349–356 **(2004)**.
[20] P.Campestrini, H.Terryn, A.Hovestad, J.H.W.de Wit; Formation of a cerium-based conversion coating on AA2024 relationship with the microstructure, Surf.Coat.Technol., **176**, 365–381 **(2004)**.
[21] L.E.M.Palomino, J.F.W.de Castro, I.V.Aoki, H.G.de Melo; Microstructural and electrochemical characterization of environmentally friendly conversion layers on aluminium alloys, J.Braz.Chem.Soc., **14(4)**, 651-659 **(2003)**.
[22] Y.Xingwen, C.Chunan, Y.Zhiming, Zh.Derui, Y.Zhongda; Study of double layer rare earth metal conversion coating on aluminum alloy LY12, Corros.Sci., **43**, 1283–1294 **(2001)**.
[23] D.K.Heller, W.G.Fahrenholtz, M.J.O'Keefe; The effect of post-treatment time and temperature on cerium-based conversion coatings on Al 2024-T3, Corros.Sci., **52**, 360–368 **(2010)**.
[24] B.R.W.Hinton, D.R.Arnott, N.E.Ryan; 'A method of forming a corrosion resistant coating', Int.Cl.4 C23C 22/48. WO 88/06639. September 7, **(1988)**.
[25] N.Mora, E.Cano, J.L.Polo, J.M.Puente, J.M.Bastidas; Corrosion protection properties of cerium layers formed on tinplate, Corros.Sci., **46**, 563–578 **(2004)**.
[26] X.Huang, N.Li, H.Wang, H.Sun, Sh.Sun, J.Zheng; Electrodeposited cerium film as chromate replacement for tinplate, Thin Solid Films, **516**, 1037–1043 **(2008)**.
[27] H.Zhang, Y.Zuo; The improvement of corrosion resistance of Ce conversion films on aluminum alloy by phosphate post-treatment, Appl.Surf.Sci., **254**, 4930–4935 **(2008)**.
[28] W.Pinc, P.Yu, M.O'Keefe, W.Fahrenholtz; Effect of gelatin additions on the corrosion resistance of cerium based conversion coatings spray deposited on Al 2024-T3, Surf.Coat.Technol., **203**, 3533–3540 **(2009)**.
[29] W.Pinc, S.Geng, M.O'Keefe, W.Fahrenholtz, T.O'Keefe; Effects of acid and alkaline based surface preparations on spray deposited cerium based conversion coatings on Al 2024-T3, Appl.Surf.Sci., **255**, 4061–4065 **(2009)**.
[30] Sh.You, Ph.Jones, A.Padwal, P.Yu, M.O'Keefe, W.Fahrenholtz, Th.O'Keefe; Response of nanocrystalline cerium-based conversion coatings on Al 2024-T3 to chloride environments, Mater.Letters, **61**, 3778–3782 **(2007)**.
[31] A.Pepe, M.Aparicio, A.Durán, S.Ceré; Recubrimientos sol gel dopados con iones Ce depositados sobre metales de aplicación industrial, Anales CONAMET/SAM, **(2004)**.
[32] A.Pepe, M.Aparicio, A.Durán, S.Ceré; Cerium hybrid silica coatings on stainless steel AISI 304 substrate, J.Sol-Gel Sci.Technol., **39**, 131–138 **(2006)**.
[33] A.Pepe, M.Aparicio, S.Ceré, A.Durán; Preparation and characterization of cerium doped silica sol–gel coatings on glass and aluminum substrates, J.Non-Cryst.Solids., **348**, 162–171 **(2004)**.
[34] N.C.Rosero-Navarro, S.A.Pellice, A.Durán, M.Aparicio; Effects of Ce-containing sol-gel coatings reinforced with SiO_2 nanoparticles on the protection of AA2024, Corros.Sci., **50**, 1283-1291 **(2008)**.
[35] K.Aramaki; Self-healing mechanism of an organosiloxane polymer film containing sodium silicate and cerium(III) nitrate for corrosion of scratched zinc surface in 0.5 M NaCl, Corros.Sci., **44**, 1621–1632 **(2002)**.
[36] K.Aramaki; Cerium(III) chloride and sodium octylthiopropionate as an effective inhibitor mixture for zinc corrosion in 0.5 M NaCl, Corros.Sci., **44**, 1361–1374 **(2002)**.
[37] K.Aramaki; Preparation of chromate-free, self-healing polymer films containing sodium silicate on zinc pretreated in a cerium(III) nitrate solution for preventing zinc corrosion at scratches in 0.5 M NaCl, Corros.Sci., **44**, 1375–1389 **(2002)**.
[38] K.Aramaki; The inhibition effects of cation inhibitors on corrosion of zinc in aereated 0.5 M NaCl, Corros.Sci., **43**, 1573-1588 **(2001)**.
[39] G.Williams, H.N.McMurray, D.A.Worsley; Cerium (III) Inhibition of Corrosion-Driven Organic Coating Delamination studied Using Scanning Kelvin Probe Technique, J.Electrochem.Soc., **149**, B154-B162 **(2002)**.
[40] K.Aramaki; Treatment of zinc surface with cerium (III) nitrate to prevent zinc corrosion in aereated 0.5 M NaCl, Corros.Sci., **43**, 2201-2215 **(2001)**.
[41] E.J.Preisler, O.J.Marsh, R.A.Beach, T.C.Mc Gill;

Stability of cerium oxide on silicon studied by X-ray photoelectron spectroscopy, J.Vac.Sci.Technol.B, **19**, 1611 **(2001)**.

[42] J.Z.Shyu, K.Otto, W.L.H.Watkins, G.W.Graham, R.K.Belitz, M.S.Gandhi; Characterization of Pd/γ-alumina catalysts containing ceria, J.Catal., **114**, 23-33 **(1988)**.

[43] H.Hoang, A.E.Hughes, T.W.Turney; An XPS study of Ru-promotion for Co/CeO_2 Fischer-Tropsch catalyst, Appl.Surf.Sci., **72**, 55-65 **(1993)**.

[44] C.V.D'Alkaine, M.N.Boucherit; Potentiostatic Growth of ZnO on Zn: Application of an Ohmic Model, J.Electrochem.Soc., **144**, 3331-3336 **(1997)**.

[45] S.Peulon, D.Lincot; Mechanistic Study of Cathodic Electrodeposition of Zinc Oxide and Zinc hydroxichloride Films from Oxigenated Aqueous Zinc Chloride Solutions, J.Electrochem.Soc., **145**, 864-874 **(1998)**.

[46] R.Guo, F.Weinberg, D.Tromans; Pitting Corrosion of Passivated Zinc Monocrystals, Corrosion, **51**, 356-366 **(1995)**.